Astronomical and Astrophysical Transactions (*AApTr*), 2024, Vol. 34, Issue 2, pp. 129–138,
ISSN 1055-6796, Photocopying permitted by license only, ©Cambridge Scientific Publishers

Modelling of the optical properties of multilayered spheroidal dust particles

D.G. Turichina[1,*], V.B. Il'in[1,2,3], V.G. Farafonov[3], S.I. Laznevoi[2]

[1] *Main (Pulkovo) Astronomical Observatory, Pulkovskoe Sh. 65/1, St. Petersburg, 196140, Russia*
[2] *St. Petersburg University, Universitetski Pr. 28, St. Petersburg, 198504, Russia*
[3] *St. Petersburg University of Aerospace Instrumentation, Bol. Morskaya Str. 67A, St. Petersburg, 190000, Russia*

Received 28 November, 2023

The approximation of cosmic dust grains by spheroids is widely used to model their optical properties. The spheroidal model combines relative simplicity, which in some cases makes it possible to find an analytical solution to the scattering problem, with sufficient flexibility in describing optical effects, including polarization. This work presents a new program able to calculate optical properties of layered spheroidal dust grains with nonconfocal concentric coaxial layers, based on the exact solution of the scattering problem by the extended boundary condition method in the spheroidal basis. The code's results are intended to be used in the modeling of the polarized light transfer through the interstellar medium with the SKIRT package.

Keywords: Scattering – polarization – ISM: dust, extinction

1 Introduction

Although such an important element influencing the radiation propagation through the Galaxy, our knowledge of the interstellar dust grains remains fairly limited. The nonsphericity of interstellar dust grains is evidenced by multiple polarimetric observations however their shape and structure are still uncertain. Coagulation in the interstellar medium might make them porous (Hirashita and Il'in 2022). On the other hand, a mantle might form around a particle core as a result of its evolution: made of carbon in the diffuse interstellar medium (Jones 2021) and ice in molecular clouds (Arslan et al. 2022).

While there is no unified interstellar dust model a few prominent recent models utilize spheroids, some of them with mantles. In particular, in THEMIS (Jones et al. 2017) particles are replaced by coated spheres, another model Astrodust (Hensley

*Email: t.dasha5@mail.ru

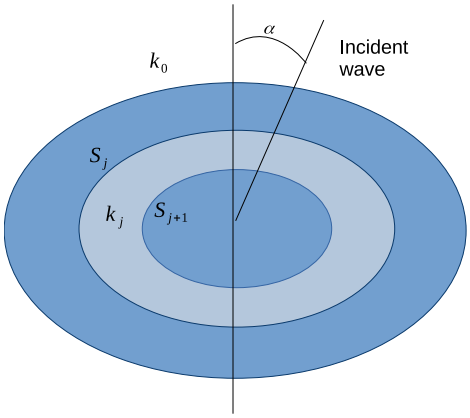


Figure 1 Multilayered spheroidal particle with coaxial and concentric layers.

and Draine 2023) assumes mixed carbon and silicate spheroidal particles. Spheroids are also included in more observationally driven models (Siebenmorgen 2023).

Naturally, spheroids get even more attention in the modeling of the polarized light transfer (Peest et al. 2023). Since the problem requires extensive calculation of the optical properties of dust in the absence of hard knowledge of particles' shapes the specific methods aimed at spheroids would be preferred to more general approaches such as Discrete Dipole Approximation (DDA) (Yurkin and Hoekstra 2011) that require more computational resources. Among others optical properties of spheroidal dust particles can be calculated with the Separation of Variables Method (SVM) (Voshchinnikov and Farafonov 1993) and the Extended Boundary Condition Method (EBCM) (Vandenbroucke et al. 2020). However, the SVM becomes unstable in the ultraviolet region (Siebenmorgen, 2018, priv. comm.) and for nonconfocal layered particles EBCM in its classical version has fundamental difficulties that prevent it from being used for layered particles altogether (Farafonov et al. 2017).

We present a new approach to the calculation of the optical properties of a single multilayered spheroidal nonconfocal dust particle based on a version of EBCM in spheroidal basis. A special feature of this method is the calculation of a special T-matrix that not only provides the required cross-sections but also simplifies its generalization to particle ensembles and integration into the process of light transfer modelling.

2 Spheroidal particle model

Polarization of scattered light is presumably mainly influenced by the ratio between the longest and shortest dimensions of a particle (Min et al. 2003). This parameter is well represented within the spheroidal model, since a spheroidal particle has two geometric parameters – the major and minor semiaxes a and b, or alternatively, their ratio a/b and the equal volume sphere radius r_v. A homogeneous particle also has an optical parameter dependent on the wavelength – the refractive index. Furthermore, the spheroidal model is relatively simple and allows us to use analytical methods.

A natural extension of this model is a layered spheroidal particle that allows us to forego the restriction of homogeneity. The j-th layer ($j = 1..N$) is supposed to be confined by two coaxial and concentric spheroidal surfaces S_j and S_{j+1}. The matter inside the j-th layer is homogeneous and isotropic with dielectric permittivity ε_j and magnetic permeability μ_j dependent only on the wavelength.

This particle interacts with a monochromatic plane wave propagating at an angle α to the particle's symmetry axis. For a given wavelength λ the wave number in each layer is $k_j = k_0\sqrt{\varepsilon_j\mu_j}$, where $k_0 = 2\pi/\lambda$ is the wave number in the vacuum.

Taking into consideration stated restrictions it is possible to solve the arising scattering problem analytically, which was done by Farafonov (2013). This work presents a code implementation and application to the problem of the polarized light scattering by a single model dust particle.

3 Scattering problem formulation

Within the EBCM the scattering process is described by the system of integro-differential equations following from the Maxwell equations considered together with the boundary conditions (Waterman 1965):

$$\vec{\nabla}\times\int_{S_j}\vec{n}\times\vec{E}^{(j)}(\vec{r}')\,G^{(j)}(\vec{r},\vec{r}')\,ds' - \frac{1}{ik_0\varepsilon_j}\vec{\nabla}\times\vec{\nabla}\times\int_{S_j}\vec{n}\times\vec{H}^{(j)}(\vec{r}')\,G^{(j)}(\vec{r},\vec{r}')\,ds' = \begin{cases} -\vec{E}_A^{(j-1)}(\vec{r}), & \vec{r}\in D_j, \\ \vec{E}_B^{(j-1)}(\vec{r}), & \vec{r}\in R^3\setminus D_j. \end{cases} \tag{1}$$

Here $E^{(j)}$ and $H^{(j)}$ are the fields in the j-th layer, D_j is the volume within S_j, $G^{(j)}$ is the Green function and $\vec{n}$ is the outer normal to S_j. In each region the fields are presented as a sum of two parts:

$$\vec{E}^{(j)} = \vec{E}_A^{(j)} + \vec{E}_B^{(j)}, \tag{2}$$

where $\vec{E}_A$ is the regular part and the irregular part $\vec{E}_B$ satisfies the radiation condition at infinity. In the outer region, where $j = 0$, $\vec{E}_A^{(0)}$ and $\vec{E}_B^{(0)}$ are none other than the incident and scattered fields.

To account for the light polarization we consider the incident radiation as a superposition of two perpendicular (TE and TM) modes with field vectors written as

$$\vec{E}^{\mathrm{in,TE}} = -\vec{i}_y\exp\left[ik_0(x\sin\alpha + z\cos\alpha)\right], \tag{3}$$

$$\vec{H}^{\mathrm{in,TE}} = \sqrt{\frac{\varepsilon_0}{\mu_0}}\left(\vec{i}_x\cos\alpha - \vec{i}_z\sin\alpha\right)\exp\left[ik_0(x\sin\alpha + z\cos\alpha)\right], \tag{4}$$

$$\vec{E}^{\mathrm{in,TM}} = \left(\vec{i}_x\cos\alpha - \vec{i}_z\sin\alpha\right)\exp\left[ik_0(x\sin\alpha + z\cos\alpha)\right], \tag{5}$$

$$\vec{H}^{\mathrm{in,TM}} = \sqrt{\frac{\varepsilon_0}{\mu_0}}\vec{i}_y \exp\left[ik_0(x\sin\alpha + z\cos\alpha)\right]. \tag{6}$$

The solutions of Eqs. (1) with either Eqs. (3)–(4) or (5)–(6) can be used to derive various optical properties of single spheroidal particles such as absorption and scattering cross-sections and the Müller matrix. To obtain such properties for a physical volume of dust they must be later averaged over the particle size, shape and orientation distributions. For this we use the package CosTuuM (Vandenbroucke et al. 2020) that already implements such averaging. Our code can be relatively easily integrated into CosTuuM thanks to the similarity between the respective solution methods.

4 T-matrix method

Our code, CosTuuM and many other codes dealing with the spheroidal particle analogues (see, for instance, Mishchenko 1991, Barber and Hill 1990) use similar methods to solve Eqs. (1). This solution involves the expansion of the incident, scattered and internal fields in a chosen functional basis with the intent to replace the integro-differential equations for fields by the linear equations for the expansion coefficients. Namely, if we expand the fields

$$\vec{E}^{(j)} = \sum_\nu a_\nu^{(j,1)} \vec{F}_\nu^{\vec{v},j}, \quad \vec{H}^{(j)} = \sum_\nu a_\nu^{(j,2)} \vec{F}_\nu^{\vec{v},j} \tag{7}$$

and substitute the expansions into Eqs. (1) it is possible to obtain the relation between the coefficient vectors for the incident and scattered fields with a matrix, widely called T-matrix

$$\vec{a}^{\,\mathrm{sca}} = T\,\vec{a}^{\,\mathrm{in}}. \tag{8}$$

This matrix contains all the information on the particle system required to calculate the optical properties. We would only need to expand the field vectors (3)–(6) in the same functions and use Eq. (8) to obtain the scattering coefficients. The cross-sections and the scattering matrix elements can all be written in terms of $\vec{a}^{\,\mathrm{sca}}$ and the base functions $\vec{F}_\nu^{\vec{v},j}$. Furthermore, the T-matrix of a particle ensemble may be analytically obtained from the single particle T-matrix. It allows easy calculation of the ensembles' optical properties in the same way it is done in the single particle case.

Since we only consider monochromatic plane waves the functions $\vec{F}_\nu^{\vec{v},j}$ must be the following solutions to the Helmholtz equation:

$$\vec{M}_\nu^{\vec{v}} = \vec{\nabla} \times (\psi_\nu\,\vec{v}), \quad \vec{N}_\nu^{\vec{v}} = \frac{1}{k}\vec{\nabla} \times \vec{M}_\nu^{\vec{v}}, \tag{9}$$

with ψ_ν being the solution of the scalar Helmholtz equation and $\vec{v}$ either a constant vector (e.g., $\vec{i}_z$) or $\vec{r}$. Electromagnetic fields must be expanded in these functions in the following form:

$$\vec{E}^{(j)} = \sum_\nu \left(a_\nu^{(j,1)}\vec{M}_\nu^{\vec{v}} + b_\nu^{(j,1)}\vec{N}_\nu^{\vec{v}}\right), \quad \vec{H}^{(j)} = \sum_\nu \left(a_\nu^{(j,2)}\vec{M}_\nu^{\vec{v}} + b_\nu^{(j,2)}\vec{N}_\nu^{\vec{v}}\right). \tag{10}$$

But there are different functional systems depending on which coordinates the equations are considered in.

The most common are spherical coordinates which yield a basis of spherical wave functions

$$\bar{\psi}_\nu(r,\theta,\varphi) = r_n(kr)\,\bar{P}_n^m(\cos\theta)\,\mathrm{e}^{im\varphi}. \tag{11}$$

In particular it is used by Vandenbroucke et al. (2020), Mishchenko (1991) and Barber and Hill (1990). Its main advantage is the relative simplicity of function calculation and distribution averaging. However, it is not well suited for larger and more elongated particles as it requires more harmonics and the numerical errors grow. Furthermore, there is an analytical limit on the outer boundary axis ratio for the layered particles above which the solution does not converge. For that reason, methods that utilize this basis usually only consider homogeneous particles.

It is also possible to use spheroidal wave functions ($n \geq m \geq 0$)

$$\bar{\psi}_\nu(\xi,\eta,\varphi) = R_{mn}(c,\xi)\,\bar{S}_{mn}(c,\eta)\,\cos m\varphi. \tag{12}$$

Here R_{mn} are the radial spheroidal functions of the first or third kind in case of the fields of the type A or B, respectively, and $\bar{S}_{mn}$ are the normalized angular spheroidal functions. The functions depend on the spheroidal coordinates and the parameter $c_j = kd_j/2$, where $d_j = \sqrt{a_j^2 - b_j^2}$ is a half of the distance between the focuses of the respective spheroidal shell, and k is either k_{j-1} or k_j depending on whether the expansion is considered outside or inside j-th layer border (see also Fig. 1). This basis is utilized by Farafonov (2013) and in this work. While there are no principal problems in spheroidal basis calculation for layered or large particles, the significant disadvantage of this method is that it requires precise spheroidal functions calculation that is relatively hard. Thankfully, this hurdle was recently overcome as the new precise procedures to calculate spheroidal functions were published by Buren (2020). They are used in our code to obtain the T-matrix and single scatterer optical properties. Through the standard transition described by Il'in et al. (2023) our "spheroidal" T-matrix can be directly transformed into a "spherical" one and averaged in CosTuuM over required distributions.

5 Solution remarks

While the solution itself is extensively presented by Farafonov (2013), it is worth considering the aspects of this solution relevant to the applications.

First and foremost, thanks to the axis symmetry of the particle the equations can be solved for different values of the azimuthal index $m = 0, 1, .., m_{max}$ independently. Hence the resulting T-matrix is a diagonal matrix of blocks each relating to the specific value of m. It simplifies the equations and reduces the memory consumption.

The formula for the resulting T-matrix can be written as follows:

$$T = A_2\,(A_1)^{-1}, \tag{13}$$

where the matrices A_1, A_2 can be obtained through the relation

$$\begin{pmatrix} A_1 \\ A_2 \end{pmatrix} = \begin{pmatrix} -\mathrm{A}_{31}^{(1)} & -\mathrm{A}_{33}^{(1)} \\ \mathrm{A}_{11}^{(1)} & \mathrm{A}_{13}^{(1)} \end{pmatrix} \cdots \begin{pmatrix} -\mathrm{A}_{31}^{(N-1)} & -\mathrm{A}_{33}^{(N-1)} \\ \mathrm{A}_{11}^{(N-1)} & \mathrm{A}_{13}^{(N-1)} \end{pmatrix} \begin{pmatrix} -\mathrm{A}_{31}^{(N)} \\ \mathrm{A}_{11}^{(N)} \end{pmatrix}. \tag{14}$$

Each $\mathrm{A}_{ik}^{(j)}$ is a 2 by 2 matrix of blocks

$$\mathrm{A}_{ik}^{(j)} = \begin{pmatrix} \alpha_{ik,1}^{(j)} & \beta_{ik,1}^{(j)} \\ \alpha_{ik,2}^{(j)} & \beta_{ik,2}^{(j)} \end{pmatrix}. \tag{15}$$

The block's elements are functions of the integrals of products of spheroidal angular functions and their derivatives which can be calculated as a sum of series (for details see Voshchinnikov and Farafonov, 1993).

The block matrix (15) is a product of two parts: $\alpha_{ik,1}^{(j)} = \bar{\alpha}_{ik,1}^{(j)} \Pi^{(j)}$ where $\bar{\alpha}_{ik,1}^{(j)}$ is the same as in the case of the confocal layer boundaries and $\Pi^{(j)}$ represents the transition between the layers that takes into account the difference in the spheroidal coordinates tied to different layer surfaces. This matrix in particular requires precisely calculated spheroidal functions, otherwise the solution may not converge when the focuses of different spheroidal layers differ significantly (for confocal particles there is no such problem since this matrix is always equal to the identity matrix).

6 Numerical results

Results of model calculations for a single particle are presented in Figs. 2–3. In the wavelength range [0.1 μm, 100 μm] we considered three types of oblate particles with the equal volume sphere radius $r_v = 0.7$ μm and the axis ratio $a/b = 2$: the homogeneous particles made of astrosilicate (Weingartner and Draine 2001), the homogeneous carbon particles (Zubko et al. 1996) and a coated particle with silicate core and a thin carbon mantle with the volume ratio $V_{\rm core}/V_{\rm total} = 0.9$. In all cases the light propagates at an angle of 45 degrees to the particle symmetry axis.

For each wavelength the maximum required values of m and n were established iteratively. In each iteration the result was obtained for $m = 0, .., m_{max}$ and $n = m, .., m + n_{max}$. The index m was increased until the next element of the sum became less than 10^{-6} of the total, n_{max} was increased until the values of $Q_{\rm ext}$ stabilized. Because of the block structure of the T-matrix we only considered the sizes of matrices n_{max} divisible by 4. Hence n_{max} was increased until the relative error of $Q_{\rm ext}$ became sufficiently small

$$\delta Q_{\rm ext} = \frac{|Q_{\rm ext}(n+4) - Q_{\rm ext}(n)|}{|Q_{\rm ext}(n+4) + Q_{\rm ext}(n)|} < 10^{-6}. \tag{16}$$

Figure 2 shows the extinction efficiency factor (i.e. the extinction cross-section divided by the geometric one) in TM mode. The efficiency factors for homogeneous particles are compared to the results obtained from CosTuuM. Both calculations were done with the expected accuracy of 10^{-6} using quadruple precision and they show agreement with the same accuracy of 10^{-6}. The other factors also in TM mode $Q_{\rm sca}$ and $Q_{\rm abs} = Q_{\rm ext} - Q_{\rm sca}$ are presented in Fig. 3. All factors decrease in parallel for longer wavelengths with a power relation representative of the Rayleigh limit and conversely merge for smaller wavelengths approaching the geometric optics region.

Figures 4 and 5 contain some technical metrics that contextualize the applicability of this solution for real life modelling. The particle size (for a given wavelength) is the main parameter that determines the time and memory required for calculations. Both

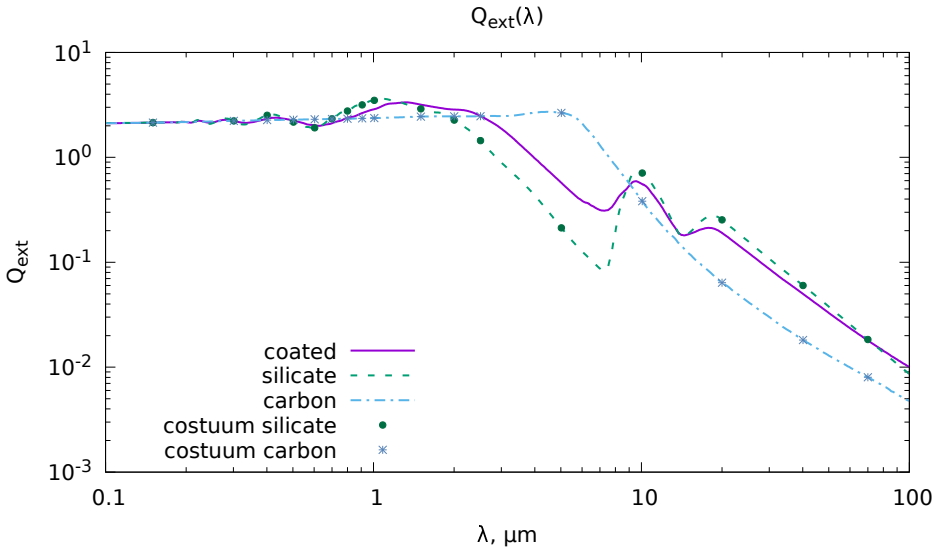


Figure 2 Extinction efficiency factors for three model oblate spheroids ($r_v = 0.7$ μm): silicate and amorphous carbon particles and coated particles with a silicate core and a thin carbon mantle ($V_{mantle}/V_{total} = 0.1$). For homogeneous particles the efficiency factors are compared to those obtained from the CosTuuM package.

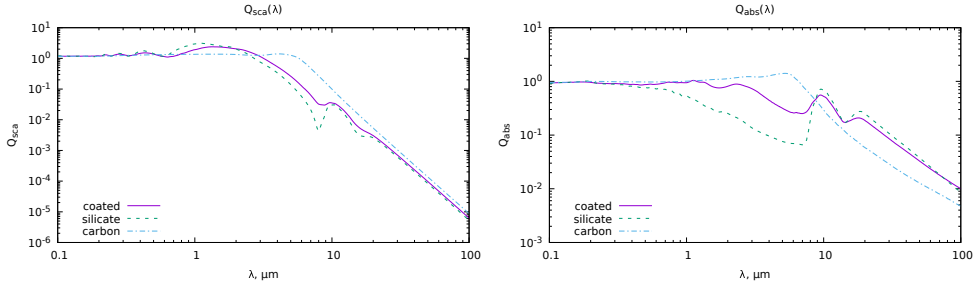


Figure 3 Scattering and absorption efficiency factors for the same particle types as in Fig. 2 depending on the wavelength.

m_{max} and n_{max} rise almost linearly with it. The value of m_{max} appears to be mostly independent of the particle structure, and small differences in n_{max} for smaller grains may be attributed to variations of the refractive index. Calculation time increases with the particle size parameter x_v as a power of about 3 to 4 for bigger particles. The solution in the spherical basis such as in CosTuuM is significantly faster for smaller particles, the solution times in spherical and spheroidal bases only become comparable for $\lambda = 0.2$ μm that corresponds to the values x_v of about 20. However, the spheroidal solution is still much faster than other methods capable of dealing with elongated and inharmonious particles such as the DDA.

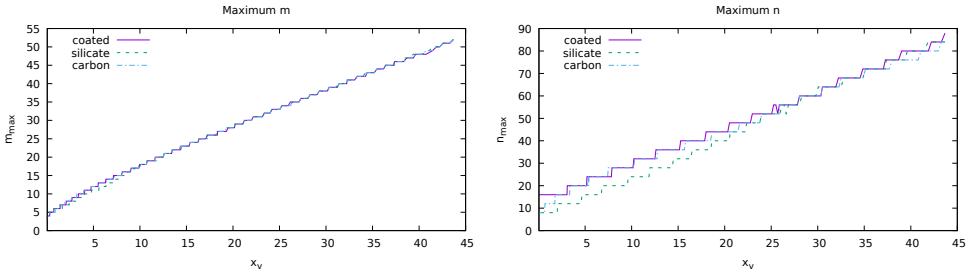


Figure 4 Values of m_{max} and n_{max} required for the convergence of the solution with accuracy 10^{-6} depending on the size parameter x_v.

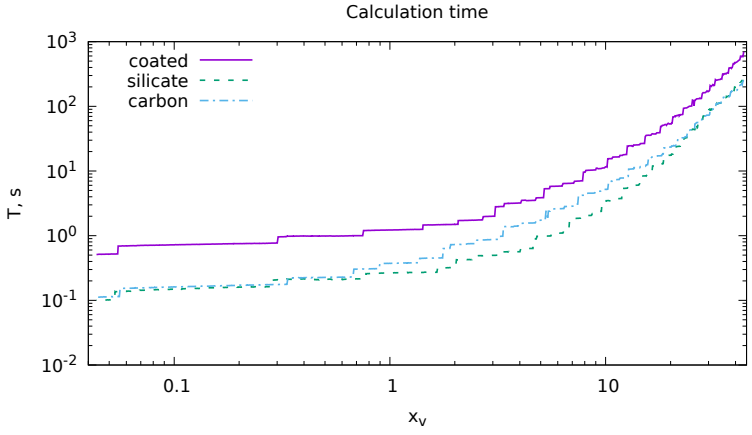


Figure 5 Time for a single particle cross-section calculation relative to the particle size parameter. Even though we have implemented parallelisation with OpenMP, for analysis all measurements were made on a single 2.7GHz core with 16Gb RAM (out of which only about 6Gb were actually used).

7 Discussion

A few scattering codes exclusively dealing with homogeneous grains have been successfully used in the polarized light transfer modelling, one prominent example being CosTuuM. The consideration of layers presents a natural next step on the path towards the physical dust models. Evidenced by Figs. 2–3 factors (or cross-sections) of homogeneous and layered particles may differ quite significantly as even a thin carbon mantle was enough to shift and smooth the 10 μm absorption band.

The presented "spheroidal" EBCM may be used to include particles with mantles, required, for example, by THEMIS into the light transfer modelling. It shows a good agreement with known solutions for the homogeneous particles and gives reasonable results for multilayered grains even if the direct validation is limited as very few existing codes can deal with layers. An important method feature is the byproduct T-matrix that allows one to integrate the solution into other EBCM versions. It was

already achieved with CosTuuM, but can also be done with other codes like MCpol by Peest et al. (2023).

The important details concerning applicability of this code for modelling are its memory and time consumption. While the memory has never been an issue in our testing, the time can be significant especially in comparison to the "spherical" methods. There are several aspects influencing the calculation time. Each multiplier in the product (14) relates to a particle layer and hence the T-matrix calculation time rises linearly with the number of layers considered. T-matrix calculation involves the series sum and a few relatively time consuming operations of matrix multiplication and inversion, hence the time is proportional to n_{max} to the power of about 3. Naturally, the time is also proportional to m_{max}. Both m_{max} and n_{max} increase almost linearly with the particle size parameter $x_v = \frac{2\pi r_v}{\lambda}$. The refractive index may also play a role in the increase of n_{max} even if it isn't as prominent for the considered particle, as most significant changes in the refractive index occur for smaller size parameters close to the Rayleigh region where the required n_{max} is small anyway.

Another crucial element of the solution is the spheroidal function calculation whose complexity significantly rises following the increase of the parameter c. Moreover, calculation of the spheroidal functions becomes much harder for the values of c with a significant imaginary part. This correlates with the increase of the absorption coefficient represented by the imaginary part of the particle refractive index and the wave number k. For such particles the numerical solution may begin to diverge due to the errors in functions calculation. The above two factors combined create twofold calculation time dependence on the x_v. For smaller x_v the function calculation takes the bulk of total time, but the bigger the matrices become, the more time is instead taken by their calculation and operations.

Nevertheless, the "spheroidal" EBCM presents a necessary working balance between the slow but versatile general methods and fast but restrictive methods for homogeneous particles.

8 Conclusion

The Extended Boundary Condition Method in spheroidal basis currently provides a nearly unique way to obtain optical properties of layered spheroidal dust grains predicted by the physical models of interstellar dust grains and required for their testing. The method is sufficiently stable and scalable and its results may be used together with other approaches to obtain the optical properties of ensembles of partially aligned non-spherical dust grains necessary for the modelling of polarized radiation transfer through the interstellar medium.

We have implemented the approach presented in a part of the package CosTuuM that prepares the data tables required to run the radiative transfer code SKIRT in its polarization mode. It opens new ways to explore cosmic dust on a global scale moving the the current constraint on the inhomogeneous spheroidal particles.

Acknowledgements

This work was supported by the RSF grant 20-72-10052.

References

[1] Arslan Ö., Hocuk S., Caselli P., et al. (2023) MNRAS 518, 2050
[2] Barber P., Hill S. (1990) Light Scattering by Particles: Computational Methods (World Scientific, Singapore)
[3] Buren A. (2020) eprint arXiv:2009.01618
[4] Farafonov V. (2013) Opt. and Spectrosc. 114, 462
[5] Farafonov V., Il'in V., Ustimov V. (2017) Adv. Math. Phys. 2017, 1
[6] Hensley B. S., Draine B. T. (2023) ApJ 948, 55
[7] Hirashita H., Il'in V. B.(2022) MNRAS 509, 5771
[8] Il'in V., Turichina D., Farafonov V., et al. (2023) JQSRT 311, 108759
[9] Jones A. P., Köhler M., Ysard N., et al. (2017) A&A 602, A46
[10] Jones A. P. (2021) eprint arXiv:2111.04516
[11] Min M., Hovenier J., de Koter A. (2003) A&A 404, 35
[12] Mishchenko M. (1991) J. Opt. Soc. Am. A 8, 871
[13] Peest C., Siebenmorgen R., Heymann F., et al. (2023) A&A 673, A112
[14] Siebenmorgen R. (2023) A&A 670, A115
[15] Vandenbroucke B., Baes M., Camps P. (2020) AJ 160, 55
[16] Voshchinnikov N. V., Farafonov V.G. (1993) Astrophys. Spa. Sci. 204, 19
[17] Waterman P. (1965) Proc. IEEE 53, 805
[18] Weingartner J., Draine B. (2001) ApJ 548, 296
[19] Yurkin M., Hoekstra A. (2011) JQSRT 112, 2234
[20] Zubko V., Mennella V., Colangeli L. et al. (1996) MNRAS, 282, 1321